Blazar-Boosted Dark Matter

Jin-Wei Wang

Astroparticle Physics, SISSA

JW Wang, A. Granelli, P. Ullio; PRL, arXiv:2111.13644

A. Granelli, P. Ullio, ***JW Wang*** ; JCAP, arXiv:2202.07598

SISSA

NCTS

Taipei, Jun 30th, 2022

Outline

- Introduction and motivation
- Spectrum of the relativistic blazar jet
- Dark matter density profile
- Dark matter flux from blazars
- Experimental constraints
- Summary

Dark matter in the Universe

- The astrophysical and cosmological observations have provided compelling evidences of the existence of **dark matter (DM)**.

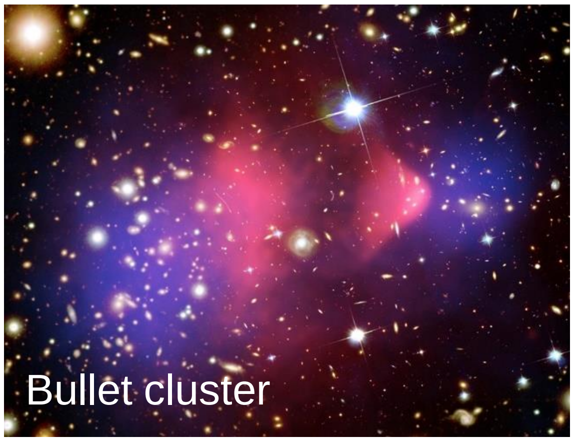

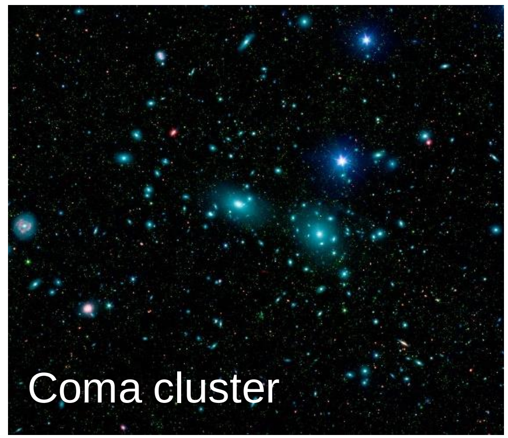

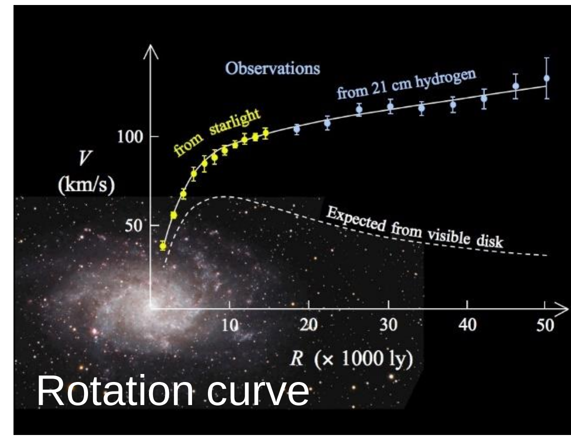

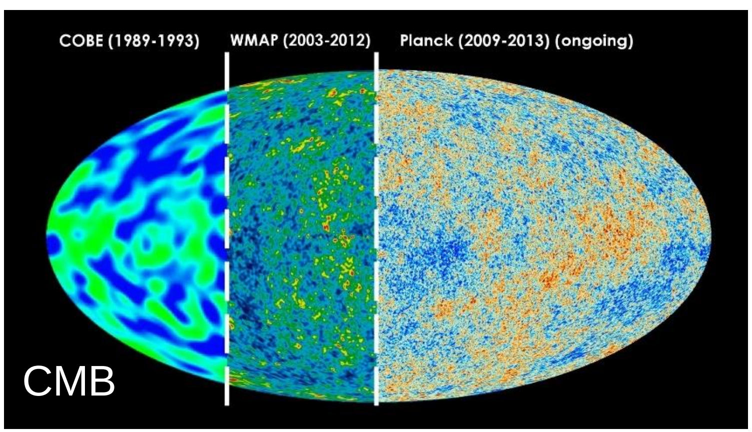

Planck 2018
[1807.06209]

Cold DM (~26%)

$$\Omega_c h^2 = 0.11933 \pm 0.00091$$

Baryons (~5%)

$$\Omega_b h^2 = 0.02242 \pm 0.00014$$

Dark energy (~69%)

$$\Omega_\Lambda = 0.6889 \pm 0.0056$$

DM direct detection

(XENON Collaboration)
Phys. Rev. Lett. 121, 111302

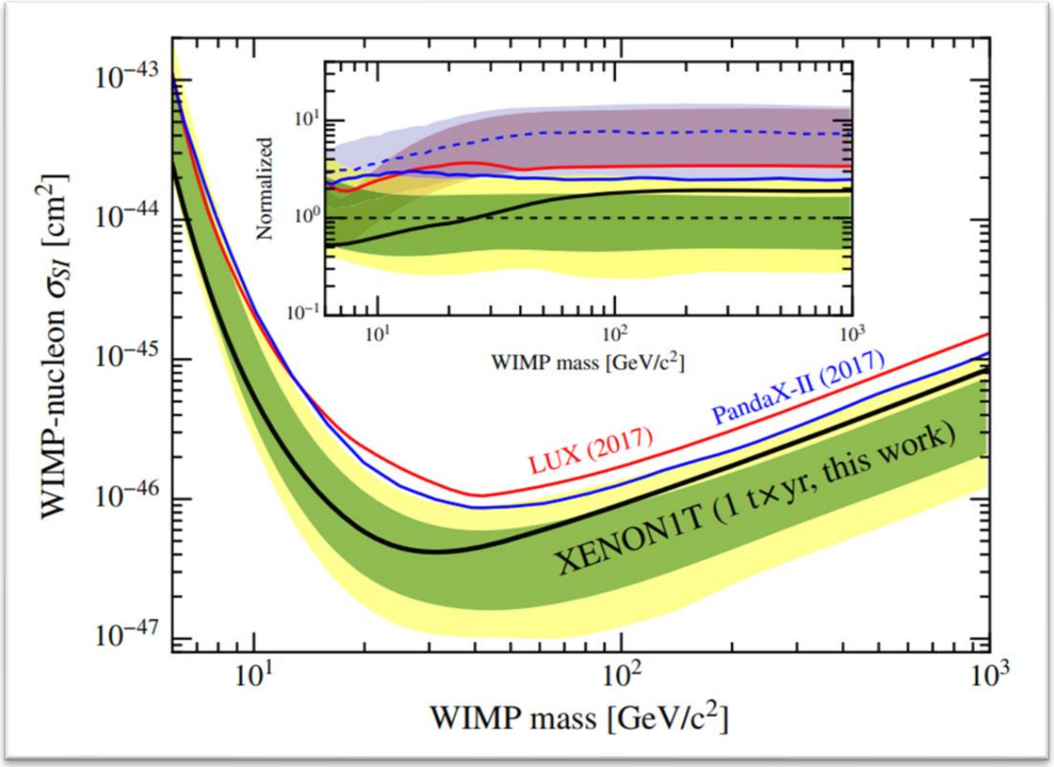

DM direct detection

(XENON Collaboration)
Phys. Rev. Lett. 121, 111302

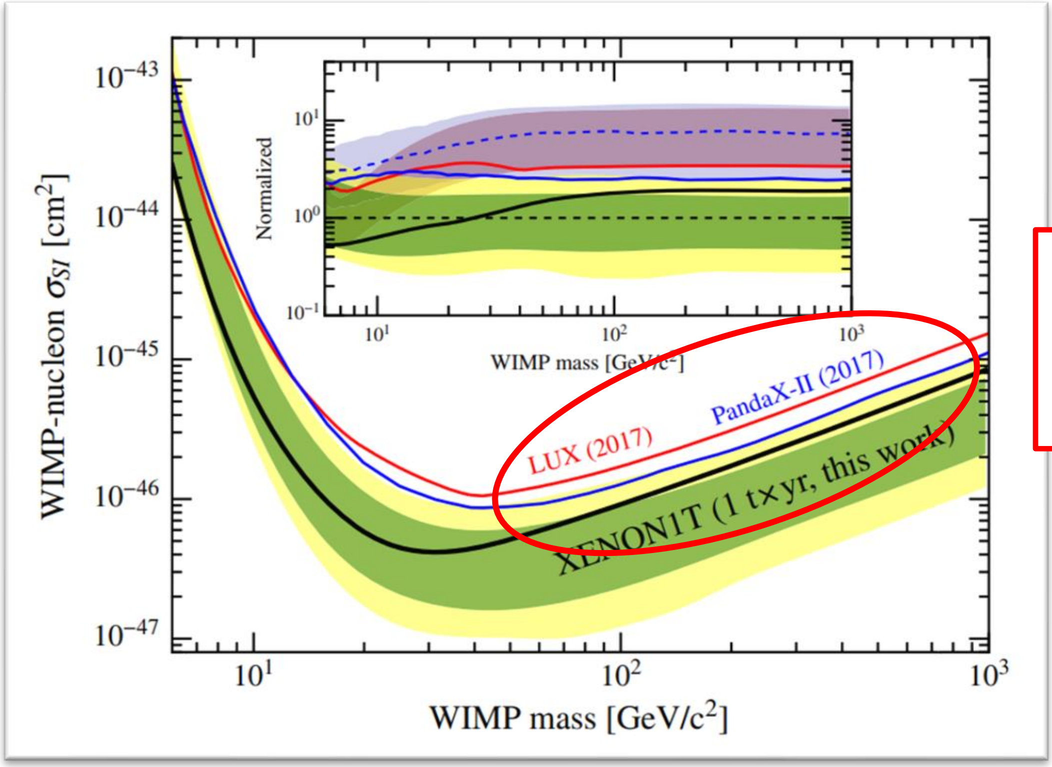

DM number density
$\sigma_{SI} \sim m_\chi$

DM direct detection

(XENON Collaboration)
Phys. Rev. Lett. 121, 111302

Kinetic energy

$E_R \in [4.9, 40.9]$ **keV**

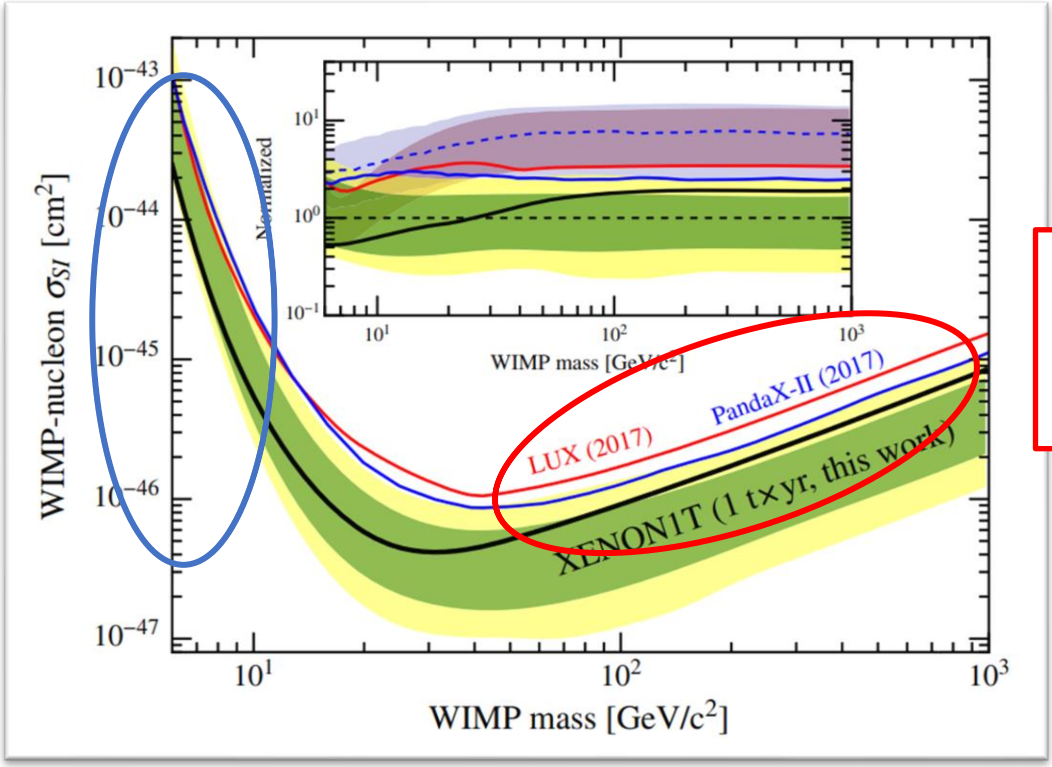

DM number density

$\sigma_{SI} \sim m_\chi$

DM direct detection

(XENON Collaboration)
Phys. Rev. Lett. 121, 111302

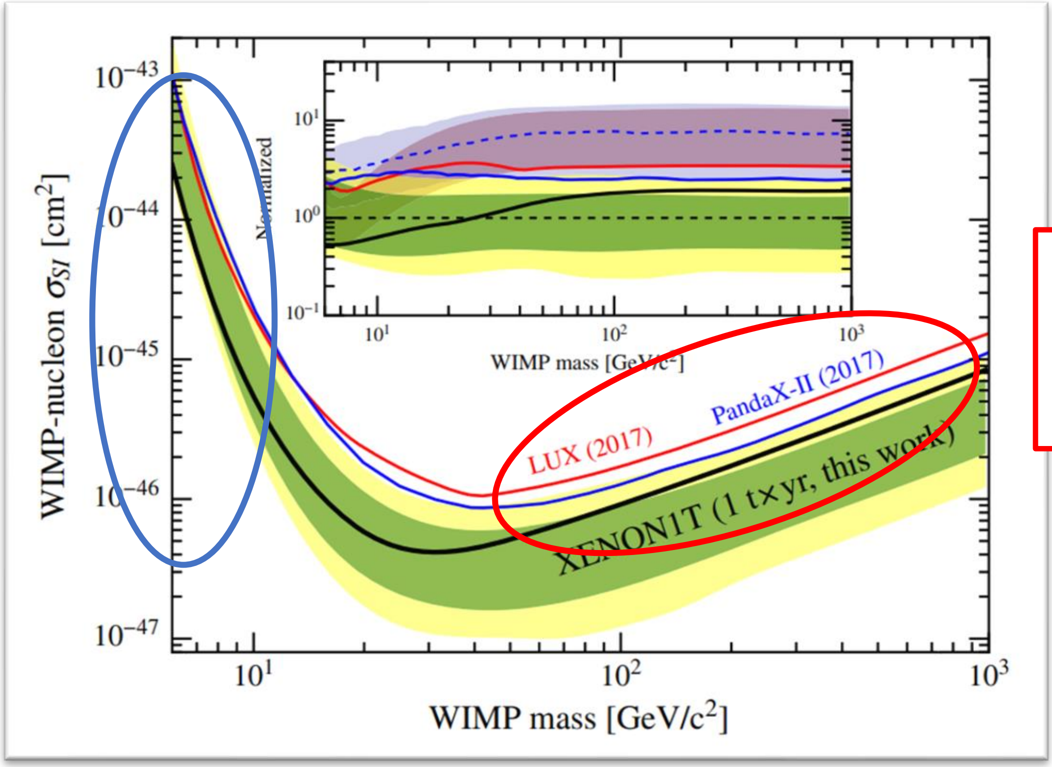

Kinetic energy

$E_R \in [4.9, 40.9]$ keV

DM number density

$\sigma_{SI} \sim m_\chi$

- **Improve DM kinetic energy:** scattering between cosmic-ray particles and DM (CRDM); [1810.10543]
- **Reduce E_{th}:** Migdal effects; [1907.11485, 1707.07258]

Why Blazars ?

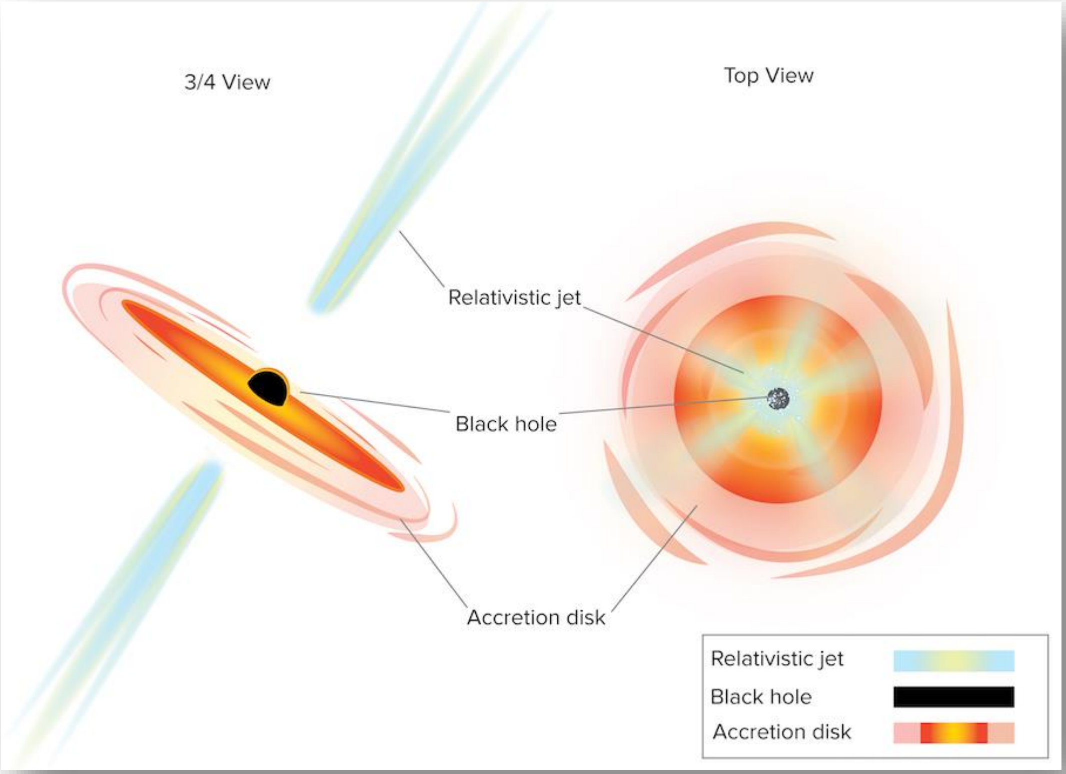

3/4 View
Top View
Relativistic jet
Black hole
Accretion disk
Relativistic jet
Black hole
Accretion disk

Why Blazars ?

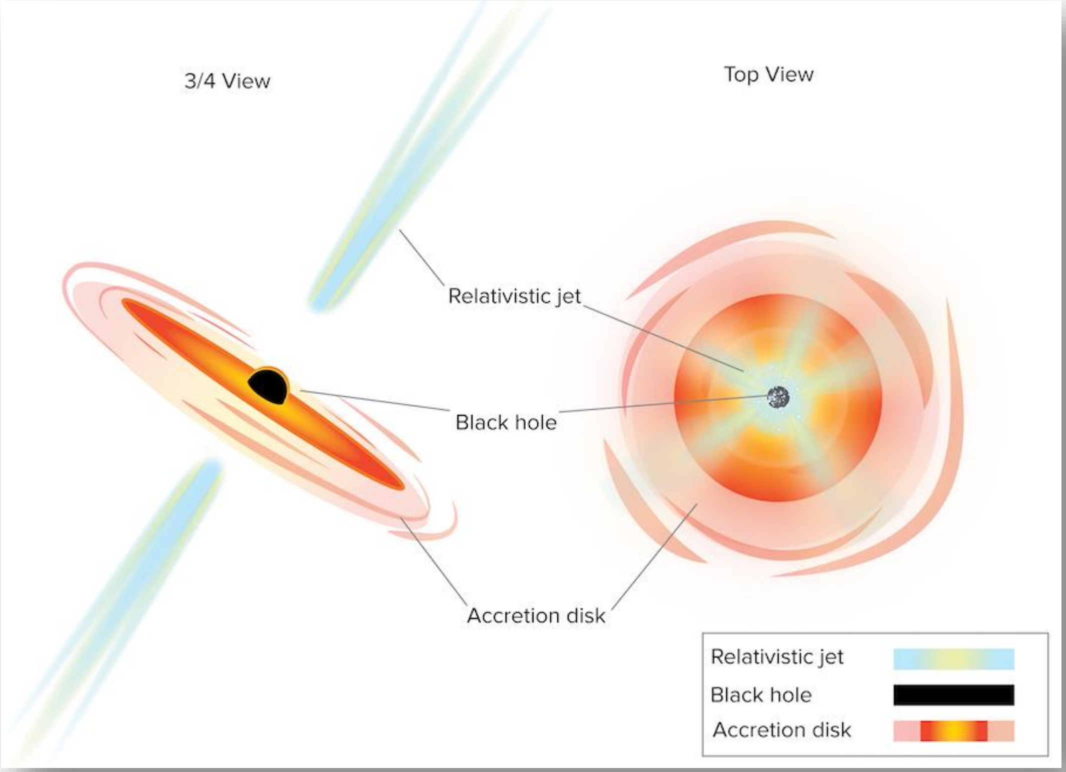

- The extremely powerful jet, which implies high proton and/or electron flux;
- Large DM density;

The blazar jet model

- **The leptonic (synchrotron-self-Compton) model**: the radio through X-ray emission is produced by electron-synchrotron radiation, while the γ-rays are produced by inverse Compton scattering;

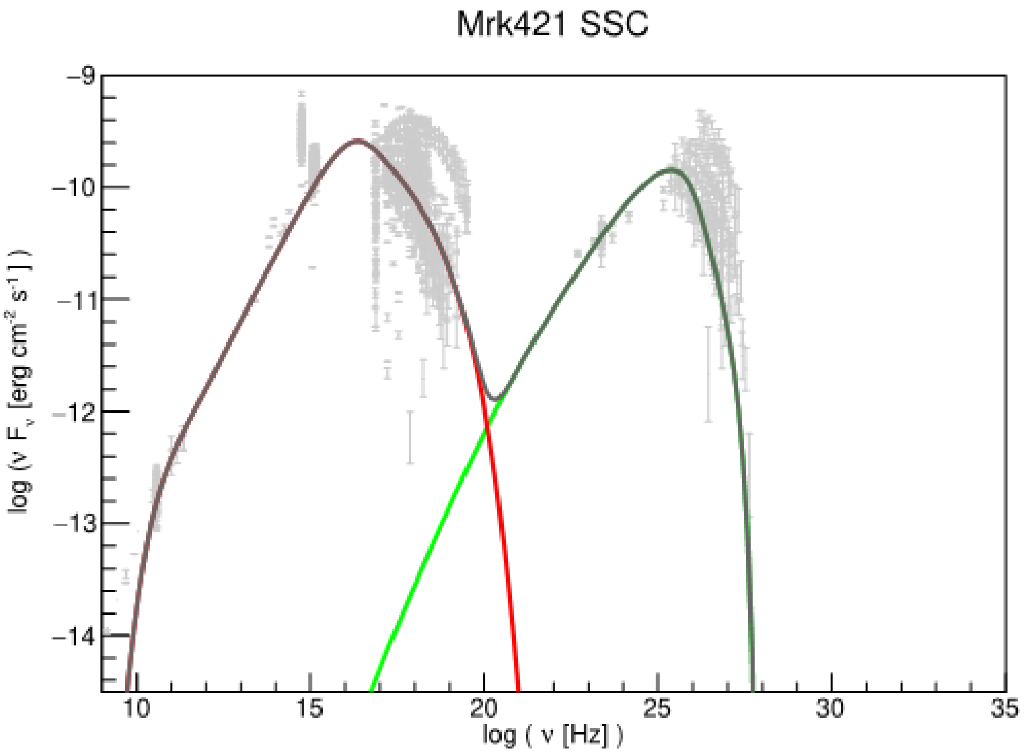

The blazar jet model

- **Pure hadronic (proton–synchrotron) model**: high-energy emission is produced by proton–synchrotron emission.

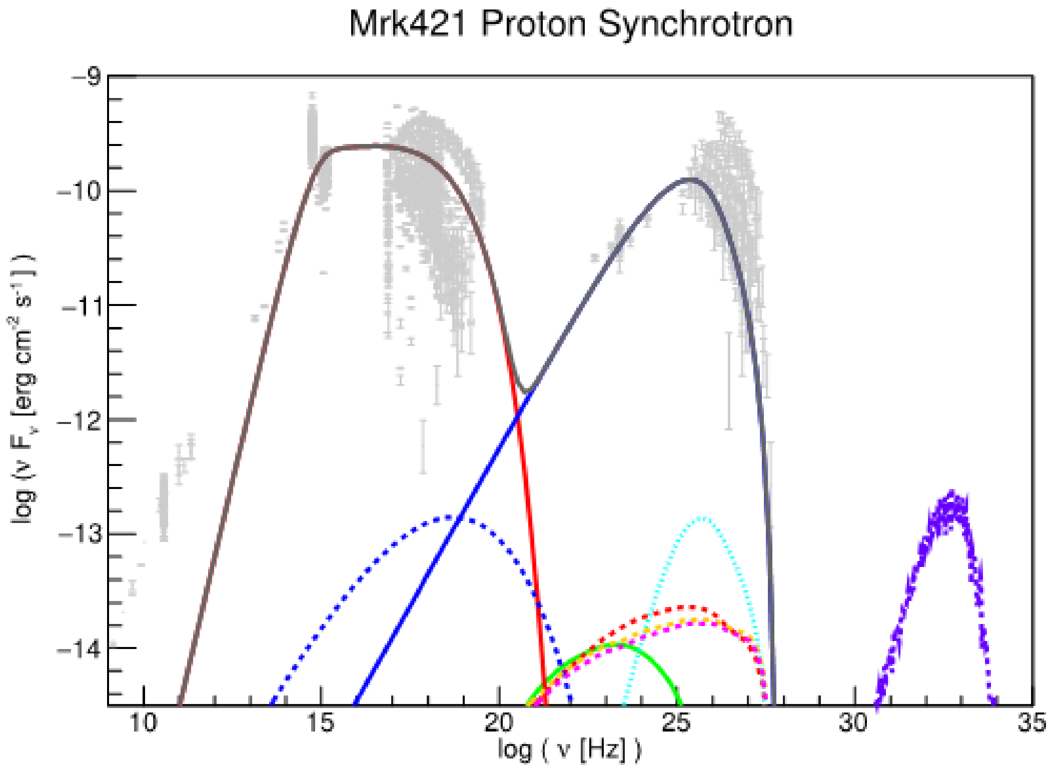

The blazar jet model

- **Lepto-Hadronic model**: high-energy emission is produced by secondary leptons produced in p-γ interactions are usually referred to as lepto-hadronic models

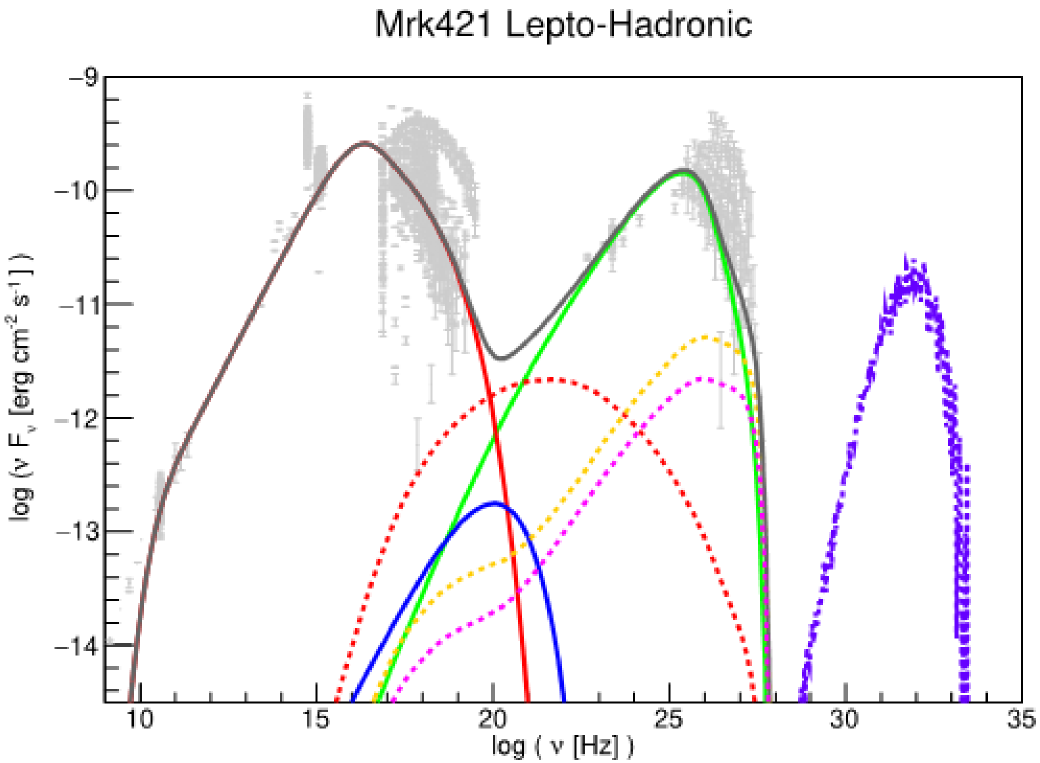

The blazar jet model

- **The leptonic (synchrotron-self-Compton) model**: the radio through X-ray emission is produced by synchrotron radiation, while the γ-rays are produced by inverse Compton scattering;
- **Pure hadronic (proton–synchrotron) model**: high-energy emission is produced by proton–synchrotron emission.
- **Lepto-Hadronic model**: high-energy emission is produced by secondary leptons produced in p-γ interactions are usually referred to as lepto-hadronic models

Photo-Meson Production

$$p + \gamma \rightarrow p' + \pi^0$$
$$p + \gamma \rightarrow n + \pi^+$$
$$p + \gamma \rightarrow p' + \pi^+ + \pi^-$$

Neutrinos as smoking gun of hadronic processes

The blazar jet model

- **The leptonic (synchrotron-self-Compton) model**: the radio through X-ray emission is produced by synchrotron radiation, while the γ-rays are produced by inverse Compton scattering;
- **Pure hadronic (proton–synchrotron) model**: high-energy emission is

In July 2018, the IceCube Neutrino Observatory announced that they have traced an extremely-high-energy neutrino back to its point of origin in the blazar TXS 0506 +056

-

hadronic models

Photo-Meson Production

$$p + \gamma \rightarrow p' + \pi^0$$
$$p + \gamma \rightarrow n + \pi^+$$
$$p + \gamma \rightarrow p' + \pi^+ + \pi^-$$

Neutrinos as smoking gun of hadronic processes

The blazar jet model

- **The leptonic (synchrotron-self-Compton) model**: the radio through X-ray emission is produced by synchrotron radiation, while the γ-rays are produced by inverse Compton scattering;
- **Pure hadronic (proton–synchrotron) model**: high-energy emission is produced by proton–synchrotron emission.
- **Lepto-Hadronic model**: high-energy emission is produced by secondary leptons produced in p-γ interactions are usually referred to as lepto-hadronic models

---

- **TXS 0506+056 lepto-hadronic model** & **BL Lacerta pure hadronic model**
- Consider the **proton/electron-DM** interaction.

Spectrum of the relativistic blazar jet

- $$\frac{d\Gamma'_j}{dE'_j d\Omega'}$$ Blob frame → $\Gamma_B \equiv (1-\beta_B^2)^{-1/2}$ Lorentz boost → $$\frac{d\Gamma_j}{dE_j d\Omega}$$ Black hole (BH) frame

Spectrum of the relativistic blazar jet

- $$\frac{d\Gamma'_j}{dE'_j d\Omega'} \xrightarrow[\text{Lorentz boost}]{\Gamma_B \equiv (1-\beta_B^2)^{-1/2}} \frac{d\Gamma_j}{dE_j d\Omega}$$

  Blob frame — Black hole (BH) frame

- Single power-law distribution: $$\frac{d\Gamma'_j}{dE'_j d\Omega'} = \frac{1}{4\pi} c_j \left(\frac{E'_j}{m_j}\right)^{-\alpha_j}$$

Spectrum of the relativistic blazar jet

- $$\frac{d\Gamma'_j}{dE'_j d\Omega'} \xrightarrow[\text{Lorentz boost}]{\Gamma_B \equiv (1-\beta_B^2)^{-1/2}} \frac{d\Gamma_j}{dE_j d\Omega}$$

  Blob frame — Black hole (BH) frame

- Single power-law distribution: $$\frac{d\Gamma'_j}{dE'_j d\Omega'} = \frac{1}{4\pi} c_j \left(\frac{E'_j}{m_j}\right)^{-\alpha_j}$$

- Lorentz boost: $$\gamma'(\gamma,\mu) = (1-\beta_B\beta\mu)\gamma\Gamma_B\,, \quad \mu'(\gamma,\mu) = \frac{\beta\mu - \beta_B}{\sqrt{(1-\beta_B\beta\mu)^2 - (1-\beta^2)(1-\beta_B^2)}}$$

with $\beta = \sqrt{1 - 1/\gamma^2}$ is the particle velocity

Spectrum of the relativistic blazar jet

- The spectrum of blazar jet in black hole frame can be expressed as:

$$\frac{d\Gamma}{dE d\Omega} = \Gamma_B \frac{d\Gamma'}{dE' d\Omega'} \left| \det \begin{pmatrix} \frac{\partial \gamma'}{\partial \gamma} & \frac{\partial \gamma'}{\partial \mu} \\ \frac{\partial \mu'}{\partial \gamma} & \frac{\partial \mu'}{\partial \mu} \end{pmatrix} \right| = \frac{d\Gamma'}{dE' d\Omega'} \frac{\beta}{\sqrt{(1-\beta\beta_B\mu)^2 - (1-\beta^2)(1-\beta_B^2)}} \, .$$

- Using the jet power to fix normalization factor c_j

$$L_j = \int d\Omega \int dT_j \, (T_j + m_j) \, \frac{d\Gamma_j}{dT_j d\Omega} = c_j m_j^2 \Gamma_B^2 \int_{\gamma'_{\min,\,j}}^{\gamma'_{\max,\,j}} d\gamma'_j \, (\gamma'_j)^{1-\alpha_j}$$

$$c_j = \frac{L_j}{m_j^2 \Gamma_B^2} \times \begin{cases} (2-\alpha_j) / \left[(\gamma'_{\max,\,j})^{2-\alpha_j} - (\gamma'_{\min,\,j})^{2-\alpha_j} \right] & \text{if } \alpha_j \neq 2 \\ 1/\log\left(\gamma'_{\max,\,j}/\gamma'_{\min,\,j}\right) & \text{if } \alpha_j = 2 \end{cases}$$

Spectrum of the relativistic blazar jet

$\mathcal{D} = 2\Gamma_B$

(Lepto-)Hadronic Model Parameters		
Parameter (unit)	TXS 0506+056	BL Lacertae
z	0.337	0.069
d_L (Mpc)	1835.4	322.7
$M_{\rm BH}$ ($M_\odot$)	3.09×10^8	8.65×10^7
$\mathcal{D}$	$40^\star$	15
Γ_B	20	15
$\theta_{\rm LOS}$ (°)	0	3.82
α_p	2.0	2.4
α_e	2.0	3.5
$\gamma'_{\rm min,\,p}$	1.0	1.0
$\gamma'_{\rm max,\,p}$	$5.5 \times 10^{7\star}$	1.9×10^9
$\gamma'_{\rm min,\,e}$	500	700
$\gamma'_{\rm max,\,e}$	$1.3 \times 10^{4\star}$	1.5×10^4
L_p (erg/s)	$2.55 \times 10^{48\star}$	9.8×10^{48}
L_e (erg/s)	$1.32 \times 10^{44\star}$	8.7×10^{42}
c_p ($\rm s^{-1}sr^{-1}GeV^{-1}$)	2.54×10^{47}	1.24×10^{49}
c_e ($\rm s^{-1}sr^{-1}GeV^{-1}$)	2.42×10^{50}	2.59×10^{54}

$\mathcal{D} = \Gamma_B$

$\theta_{\rm LOS} \simeq 1/\mathcal{D}$

Spectrum of the relativistic blazar jet

- Spectrum in BH frame:

$$\frac{d\Gamma_j}{dT_j d\Omega} = \frac{1}{4\pi} c_j \left(1 + \frac{T_j}{m_j}\right)^{-\alpha_j} \frac{\beta_j (1 - \beta_j \beta_B \mu)^{-\alpha_j} \Gamma_B^{-\alpha_j}}{\sqrt{(1 - \beta_j \beta_B \mu)^2 - (1 - \beta_j^2)(1 - \beta_B^2)}}$$

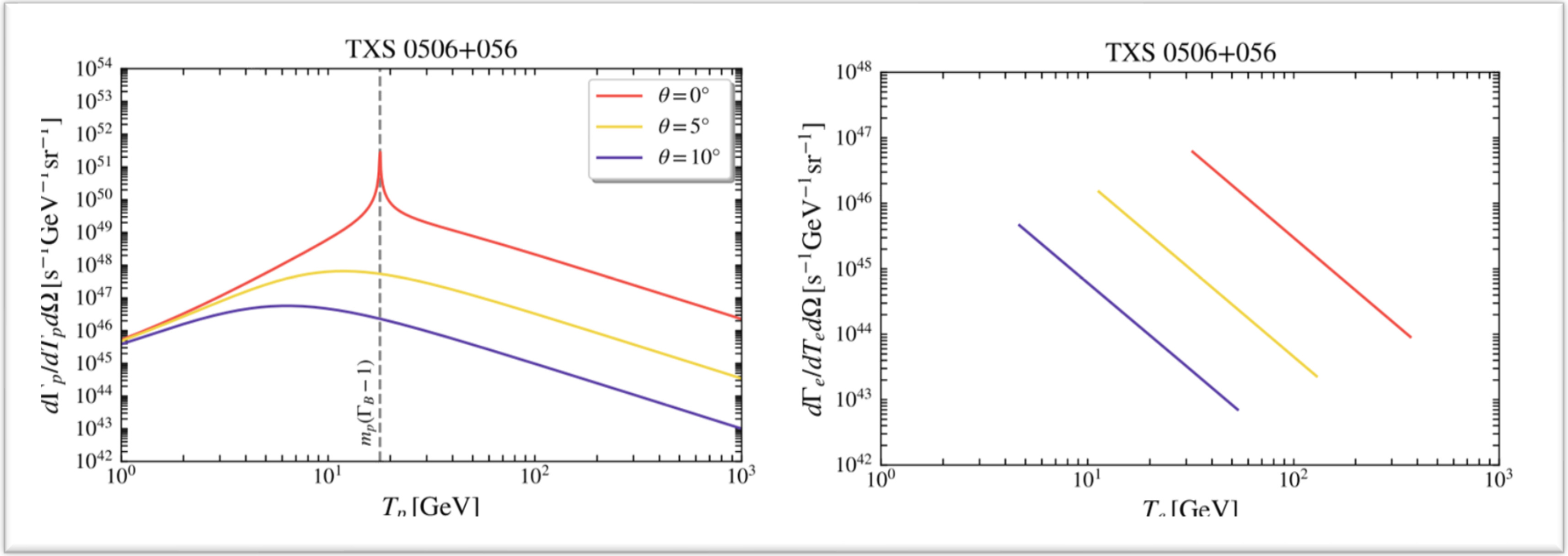

Dark matter density profile

- The DM distribution depends on the properties of central supermassive black hole;

$$\rho(r) \propto r^{-\gamma} \xrightarrow{\text{Adiabatic growth}} \rho'(r) \propto r^{-\frac{9-2\gamma}{4-\gamma}}$$

Set $\gamma = 1$, which corresponds to the NFW profile

Dark matter density profile

- The DM distribution depends on the properties of central supermassive black hole;

$$\rho(r) \propto r^{-\gamma} \quad \xrightarrow{\text{Adiabatic growth}} \quad \rho'(r) \propto r^{-\frac{9-2\gamma}{4-\gamma}}$$

Set $\gamma = 1$, which corresponds to the NFW profile

- The possible DM annihilations could flatten the DM profile in the inner region

$$\rho_{\rm core} \simeq m_\chi / (\langle \sigma v \rangle_0 t_{\rm BH}) \quad \xrightarrow{\text{Annihilation}} \quad \rho_{\rm DM}(r) = \frac{\rho'(r)\rho_{\rm core}}{\rho'(r) + \rho_{\rm core}}$$

Dark matter density profile

- The DM distribution depends on the properties of central supermassive black hole;

$$\rho(r) \propto r^{-\gamma} \xrightarrow{\text{Adiabatic growth}} \rho'(r) \propto r^{-\frac{9-2\gamma}{4-\gamma}}$$

Set $\gamma = 1$, which corresponds to the NFW profile

- The possible DM annihilations could flatten the DM profile in the inner region

$$\rho_{\rm core} \simeq m_\chi/(\langle\sigma v\rangle_0\, t_{\rm BH}) \xrightarrow{\text{Annihilation}} \rho_{\rm DM}(r) = \frac{\rho'(r)\rho_{\rm core}}{\rho'(r)+\rho_{\rm core}}$$

- The normalization condition to fix the DM profile

$$\int_{4R_S}^{10^5 R_S} 4\pi r^2 \rho'(r)dr \simeq M_{\rm BH}$$

Where R_S is Schwarzschild radius

Dark matter density profile

- Consider two benchmark points

$$\text{BMP1) } \langle \sigma v \rangle_0 = 0, \text{ so that } \rho_{\rm core} \to +\infty \text{ and } \rho_{\rm DM} = \rho';$$
$$\text{BMP2) } \langle \sigma v \rangle_0 = 10^{-28}\,{\rm cm^3\,s^{-1}} \text{ and } t_{\rm BH} = 10^9\ {\rm yr};$$

- DM profile

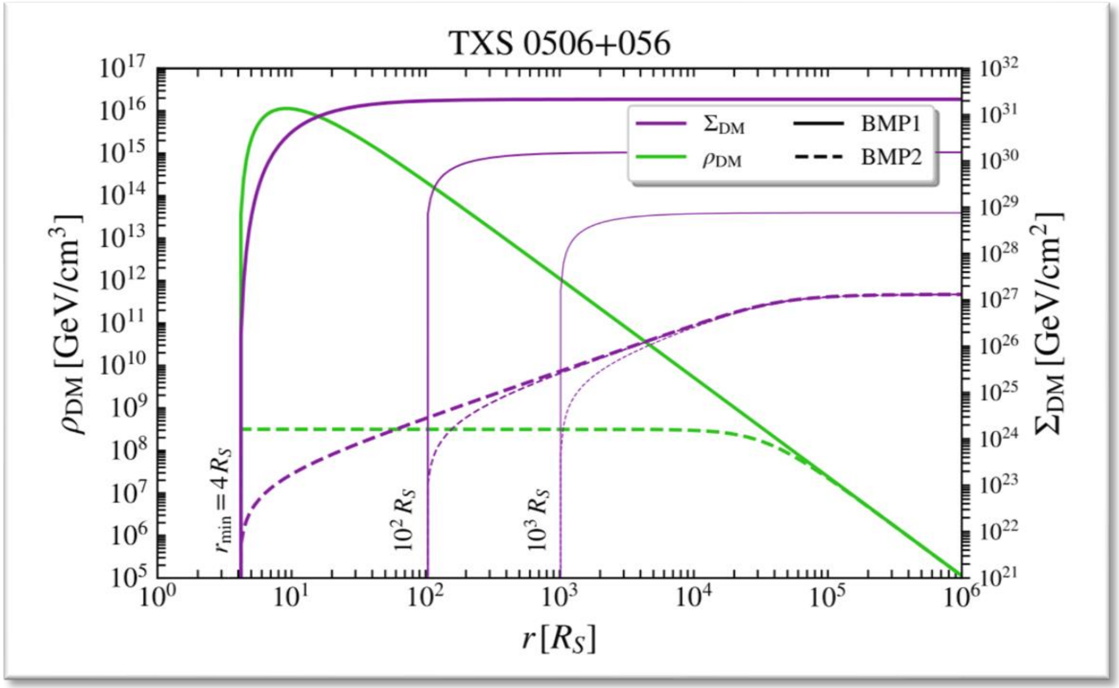

- The line-of-sight integral of DM density

$$\Sigma_{\rm DM}(r) \equiv \int_{r_{\rm min}}^{r} \rho_{\rm DM}(r')\,dr'$$

Dark matter flux from blazars

- The BBDM flux can be expressed as

$$\frac{d\Phi_\chi}{dT_\chi} = \frac{\Sigma_{\rm DM}^{\rm tot}\,\widetilde{\sigma}_{\chi p}}{2\pi m_\chi d_L^2} \int_0^{2\pi} d\phi_s \int_{T_p^{\rm min}(T_\chi)}^{T_p^{\rm max}} \frac{dT_p}{T_\chi^{\rm max}(T_p)} \frac{d\Gamma_p}{dT_p d\Omega}$$

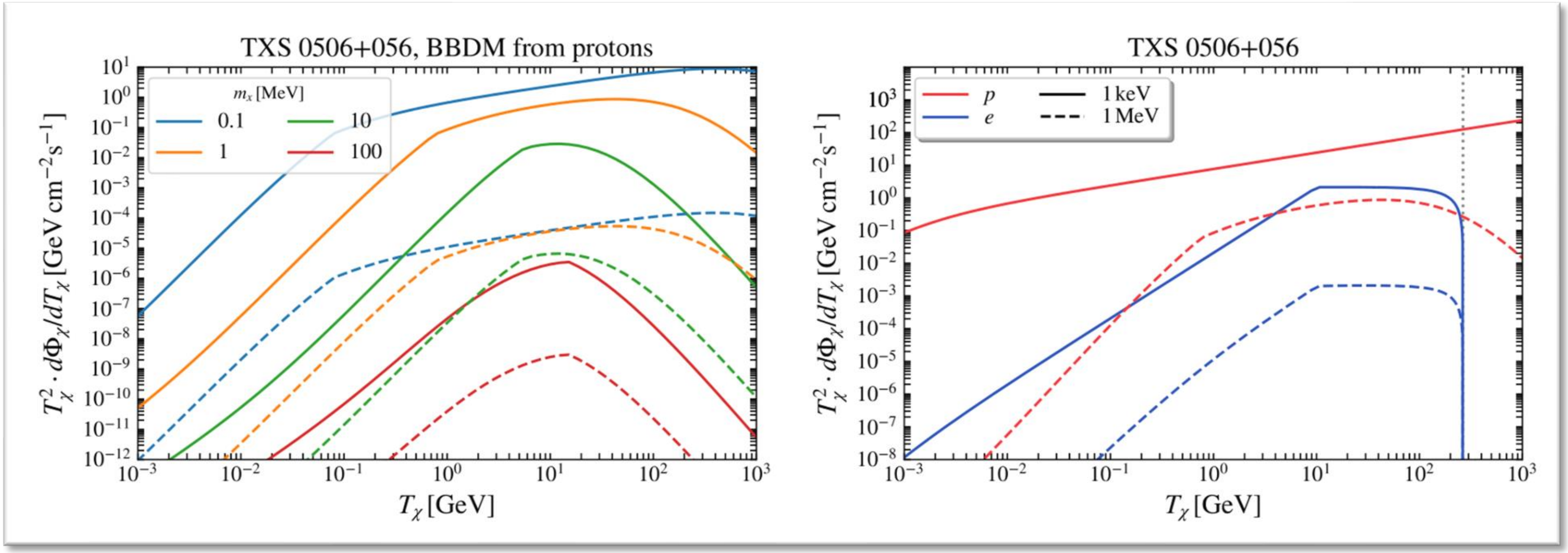

Direct detection constraints

- The BBDM-induced target nucleus (electron) recoil rate can be expressed as

$$\Gamma_j^{\rm DM} \simeq \int_{T_{\rm exp}^{\rm min}}^{T_{\rm exp}^{\rm max}} dT_j \, \tilde{\sigma}_{\chi j} \int_{T_\chi^{\rm min}(T_j)}^{+\infty} \frac{dT_\chi}{T_j^{\rm max}(T_\chi)} \frac{d\Phi_\chi}{dT_\chi} \quad (\text{with } j = e,\ N)$$

- For Xenon1T (SI): $\Gamma_N(4.9\ \mathrm{keV} \leq T_{\rm Xe} \leq 40.9\ \mathrm{keV}) < 2.41 \times 10^{-34}\ \mathrm{s}^{-1}$

For Borexino (SD): $\Gamma_{\rm p}(T_p > 25\ \mathrm{MeV}) < 2 \times 10^{-39}\ \mathrm{s}^{-1}$

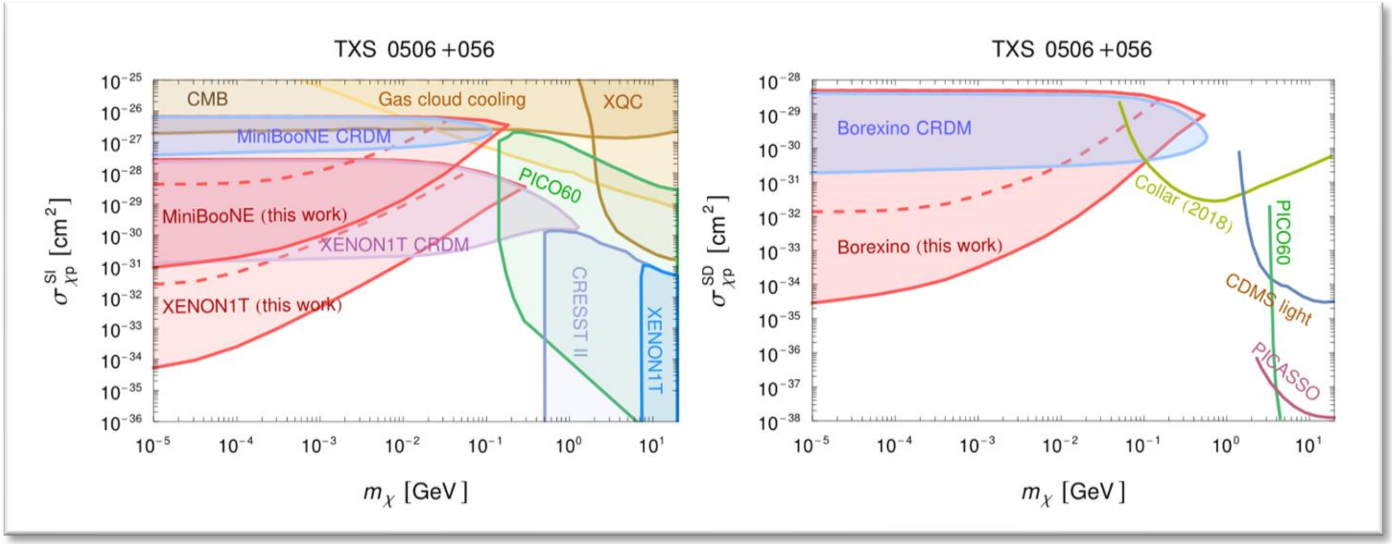

Constraints from Super-K

- Due to the large volume (22.5 kt in fiducial volume) and long exposure time (2628.1 days), Super-K is an ideal detector to search for DM-electron scattering signals.

- Three energy bins are considered, and the spatial distribution of the events are also given.

$$P\left(\mu_e > \cos\delta;\, T_\chi^{\min}(T_e = T_l^{\min})\right) \gtrsim 0.95$$

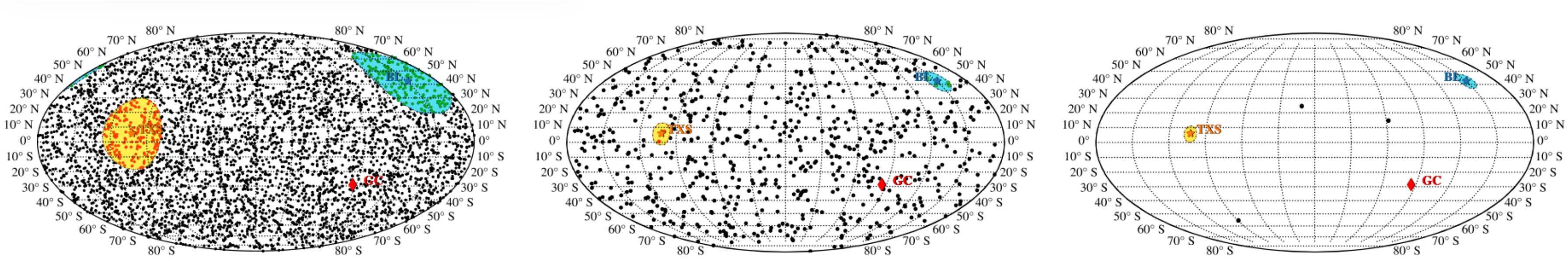

$0.1 < T_e/\mathrm{GeV} < 1.33$ $\quad$ $1.33 < T_e/\mathrm{GeV} < 20$ $\quad$ $20 < T_e/\mathrm{GeV} < 10^3$

Constraints from Super-K

- After doing a Poisson analysis, we derive the 95% C.L. upper limits

Sensitivity of Super-Kamiokande			
	Bin1	Bin2	Bin3
T_e (GeV)	$(0.1,\ 1.33)$	$(1.33,\ 20)$	$(20,\ 10^3)$
$N_{\rm Data}$	4042	658	3
$N_{\rm Bkg}$	3992.9	772.6	7.4
$\epsilon_{\rm sig}$	93.0%	91.3%	81.1%
δ	24°	7°	5°
$N^\delta_{\rm TXS}$	169	2	0
$N^\delta_{\rm BL}$	167	4	0
$N^\delta_{\rm Bkg}$	172.6	2.88	0.014
$N_{\rm TXS}$ (95% C.L.)	19.39	3.42	2.98
$N_{\rm BL}$ (95% C.L.)	17.27	6.27	2.98

- The number of BBDM-induced electron recoil events at Super-K

$$N_e^{\rm DM} \simeq N_e \sigma_{\chi e} t_{\rm obs} \int_{T_{\rm exp}^{\rm min}}^{T_{\rm exp}^{\rm max}} dT_e \int_{T_\chi^{\rm min}(T_e)}^{+\infty} \frac{dT_\chi}{T_e^{\rm max}(T_\chi)} \frac{d\Phi^z_\chi}{dT_\chi}$$

$$N_e^{\rm DM} \times \epsilon_{\rm sig} < N_{\rm TXS}\,(N_{\rm BL})$$

Constraints from Super-K

- Combing three bins, we derive the 95% C.L. upper limits on $\sigma_{\chi e}$

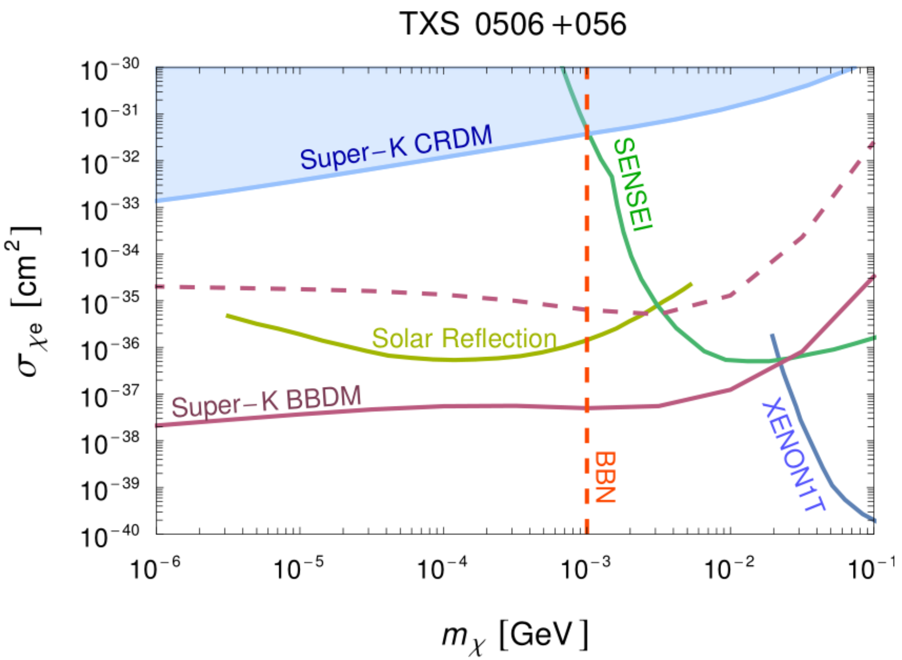

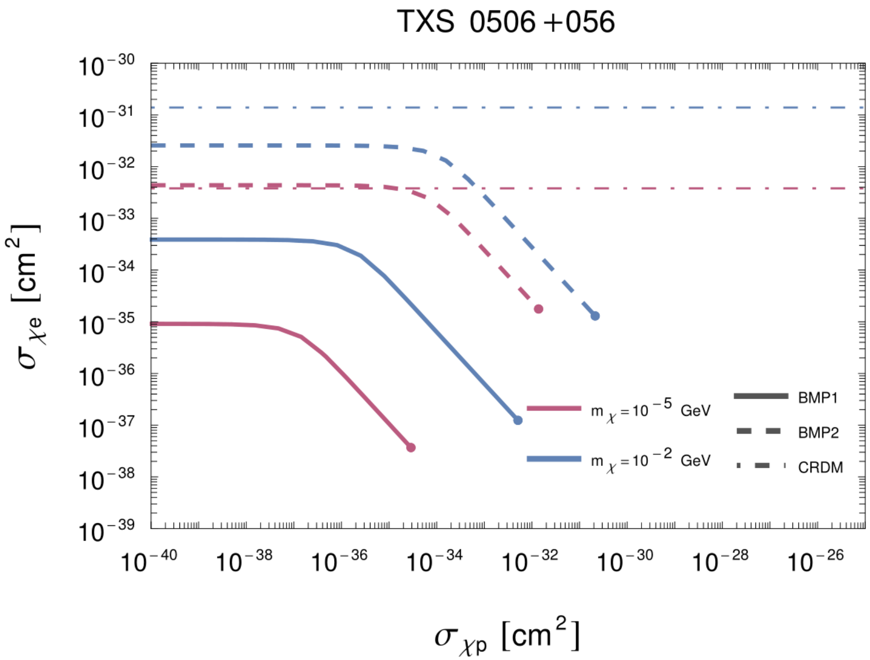

- Left: fix $\sigma_{\chi p}$ with XENON1T constraints; Right: for various $\sigma_{\chi p}$.

Summary

- A novel astrophysical mechanism for DM acceleration;
- Due to the powerful jets and large DM densities, the blazars are ideal DM boosters and can induce a stronger DM flux than that from CRs;
- The strong constraints on $\sigma_{\chi p}$ and $\sigma_{\chi e}$ are derived by using the results of XENON1T and Super-K;
- It not only unveils a novel fascinating possibility to explore the nature of DM but also provides astrophysicists with a new way to better understand the characteristics of blazar jets.

Summary

- A novel astrophysical mechanism for DM acceleration;
- Due to the powerful jets and large DM densities, the blazars are ideal DM boosters and can induce a stronger DM flux than that from CRs;
- The strong constraints on $\sigma_{\chi p}$ and $\sigma_{\chi e}$ are derived by using the results of XENON1T and Super-K;
- It not only unveils a novel fascinating possibility to explore the nature of DM but also provides astrophysicists with a new way to better understand the characteristics of blazar jets.

Thank you